INTERNATIONAL JOURNAL OF PRECISION ENGINEERING AND MANUFACTURING Vol. 13, No. 11, pp. 2043-2049 NOVEMBER 2012 / 2043
DOI: 10.1007/s12541-012-0269-y

Gait Cycle Comparions of Cruciate Sacrifice for Total Knee Design.-Explicit Finite Element

Kyoung-Tak Kang[1,*], Joon-Hee Park[2,*], Kwang-Il Lee[3,4], Young-Bock Shim[3], Ju-Woong Jang[3], and Heoung-Jae Chun[1,#]

1 School of Mechanical Engineering, Yonsei University, Seoul, Korea, 120-749
2 Department of Anesthesiology & Pain Medicine, Kangdong Sacred Heart Hospital, Hallym University College of Medicine, Seoul, Korea, 134-814
3 The Institute of Biomater & Medical Eng, Korea Bone Bank Co, Ltd, Seoul, Korea, 153-802
4 Brain Korea 21 Project for Medical Science, Yonsei University, Seoul, Korea, 120-749
Corresponding Author / E-mail: hjchun@yonsei.ac.kr, TEL: +82-2-2123-4827, FAX: +82-2-2123-2736
* Kyoung-Tak Kang and Joon-Hee Park contributed equally to this work

KEYWORDS: Finite element method, Total knee replacement, Gait cycle

Joint kinematics and contact mechanics dictate the success of current total knee replacement (TKR) devices. Computational contact prediction is a feasible way of evaluating new TKR designs prior to physical testing and implementation. Previous finite element (FE) knee models have generally been used to predict stresses on contact areas and/or areas subjected to static or quasi-static loading. Explicit dynamic FE analyses have recently been used to effectively predict TKR kinematics and contact mechanics during dynamic loading conditions. In this study, we compared the functional load transmission and kinematic performance of two posterior-stabilized designs, standard and post-cam TKR versions, over a standardized loading cycle using three-dimensional contact finite element analysis. Our objective was to develop and experimentally validate an explicit FE TKR model that incorporates femoral-bearing articulations. Finite element-based computational contact pressure predictions were applied to gait cycles using both force-controlled and displacement-controlled inputs. A standard prosthesis showed a reduction in contact pressure compared with post-cam prosthesis components, as it redistributed the knee motion to two articulating interfaces with more linear motions at each interface. In this FE analysis, the wear of TKR bearings was dependent on kinematics at the articulating surfaces and on prosthesis design.

Manuscript received: February 1, 2012 / Accepted: June 25, 2012

1. Introduction

Improvements in total knee replacement (TKR) designs, materials, and sterilization techniques during the past decade have led to improved clinical performance of knee prostheses by reducing the prevalence of delamination and structural fatigue of the ultra high molecular weight polyethylene (UHMWPE) bearings.[1,3] Long-term performance of TKR components is influenced by joint kinematics and contact mechanics. The combination of contact stresses and relative motion contributes to wear and fatigue damage of the implant. In vitro studies have quantified the importance of kinematic conditions and contact pressure and area on wear.[4,5] Total knee replacements are subjected to millions of loading cycles in vivo, and damage has been observed at the surface of retrieved polyethylene tibial components,[6] which has raised some concerns about the longevity of total knee replacements.[7] Wear affecting total knee replacements can include a wide range of surface damage modes, including permanent deformation, embedded third body debris, scratching, abrasion, burnishing, pitting, and delamination of the polyethylene tibial component. Thus, tibial components exhibit contact fatigue, adhesive and abrasive wear, and wear due to a third body in vivo. The generation of UHMWPE wear debris from articulating surfaces in total knee replacements is affected by a number of factors. Using analytical and finite element (FE) techniques, Bartel et al.[8] proposed that surface damage in tibial components was associated with stresses in the polyethylene generated at the articulating surface.

FE analyses of increasing complexity have been developed over the past two decades to evaluate the bearing stresses in tibial inserts (bearing).[9-11] Recently, Sathasivam and Walker[12] studied the effect of surface bearing geometry on tibial insert stresses using decoupled kinematic and FE analyses of a total knee replacement. First, a rigid body analysis was used to determine the position of the femur at discrete intervals during the stance phase of gait. Next, the predicted kinematics was applied to a finite element model of a total knee replacement to determine the stresses in the polyethylene bearing. The authors concluded that proper simulation of the joint kinematics was crucial. An important limitation of this work, however, was that

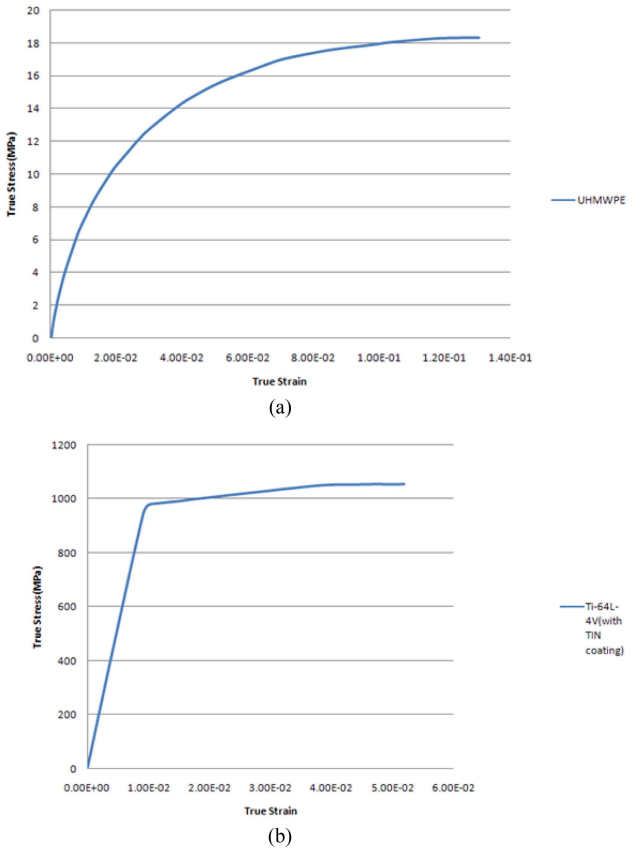

Fig. 1 Material properties (a) UHMWPE (b) Ti-641-4V (with TIN coating)

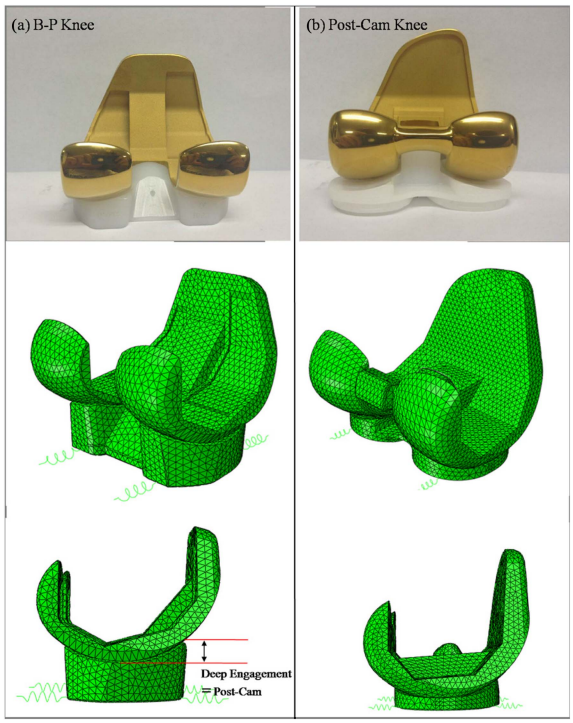

Fig. 2 Finite element models for (a) B-P Knee and (b) Post-Cam Knee

only linear elastic material properties were considered for the polyethylene. Plasticity plays a fundamental role in the mechanical behavior of polyethylene when subjected to the loading conditions prevalent in total knee replacements.[13] However, due to the complexity introduced by including plastic flow behavior for polyethylene, the coupling of kinematics and stress analyses for total joint replacement has not been explored extensively in the literature.

In general, implicit FE analyses have been utilized to predict contact mechanics during a single static loading or series of static positions, but lack the ability to predict relative motion during a force-controlled analysis and represent only the simplest loading conditions. Recently, explicit dynamic FE analyses that are able to efficiently determine joint and contact mechanics simultaneously during dynamic loading conditions have been used to develop dynamic models of insert-femoral contact.[14,15] The tibia-femoral kinematics of the model during a force-controlled gait simulation was verified by comparisons with data from an experimental knee simulator.

The objective of the present study was to develop and experimentally validate an explicit FE model of a TKR including bearing-femoral articulations. The plastic characteristics of UHMWPE materials were considered in the FE model. The contact stress was calculated for posterior-stabilized B-P Knee (Korea Bone Bank Co., Ltd., Seoul) and Post-Cam Knee (Endotec Inc., Orlando, FL, USA) designs without considering differences between mobile and fixed bearings. Loading conditions were the normal level walking for both B-P knee and Post-Cam knee models.

2. Materials and Methods

2.1 Material Properties

A unique feature of the B-P Knee design is the TiN coating on the Ti-6AL-4V. The plasticity model and titanium TiN coating model were used as elements representing a polyethylene bearing, and tensile tests were carried out according to ASTM D-638 guidelines. Titanium femoral tensile tests were carried out according to ASTM F-2516 guidelines in an MTS 810.23 servo-hydraulic testing system (Fig. 1). The Post-Cam Knee was made of cobalt-chrome (Young's modulus, 220 GPa; Poisson's ratio, 0.3).[16]

2.2 Explicit FE Model

The posterior-stabilized design of B-P Knee was to be unique characteristic for bearing to have deep engagement. In general, for posterior-stabilized designs for TKR, the design, with post-cam substituting posterior cruciate ligament, was widely used. However, in B-P Knee, the region for deep engagement in bearing replaced the post-cam (Fig. 2). FE models of both the B-P Knee and Post-Cam Knee were used in fully three-dimensional, materially and geometrically nonlinear, large displacement, multiple contact surface formulations (Fig. 2).

Solid modeling and meshing was performed using Hypermesh 10.0 (Altair Engineering, Inc., Troy, MI, USA), and analysis and post-processing was performed using ABAQUS 6.10 (Abaqus, Inc., Providence, RI, USA). The formulation generates a fully dynamic model that is able to predict knee motions and polyethylene stresses when loaded in a gait cycle (Fig. 3).

The bearing and femoral were meshed using second order 10-noded, three-dimensional triangular elements. Bearing element edge

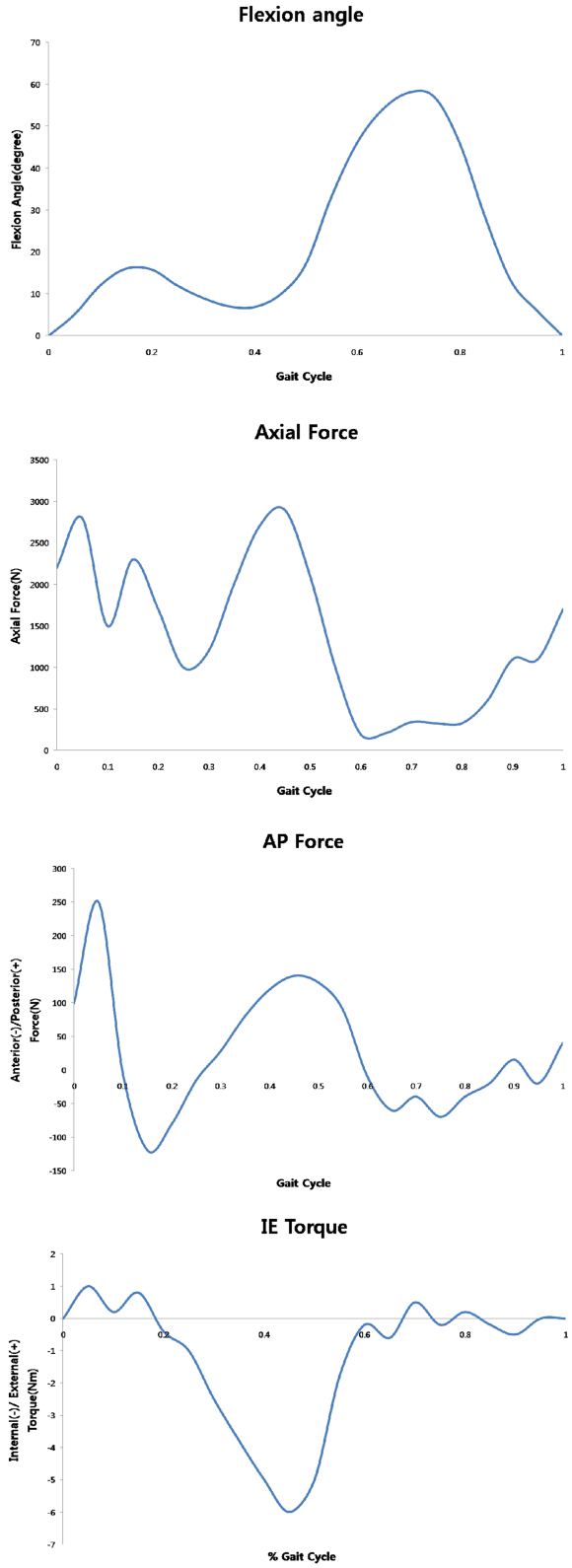

Fig. 3 Knee wear simulator and finite element model inputs: flexion angle, axial force, AP force and IE torque

lengths were determined in prior convergence studies under similar conditions.[17,18] The coefficient of friction between the articulating surfaces was assumed to be 0.07, in agreement with the ranges reported in the literature.[12] A penalty-based method was employed to define contact. The non-linear pressure-overclosure relationship was

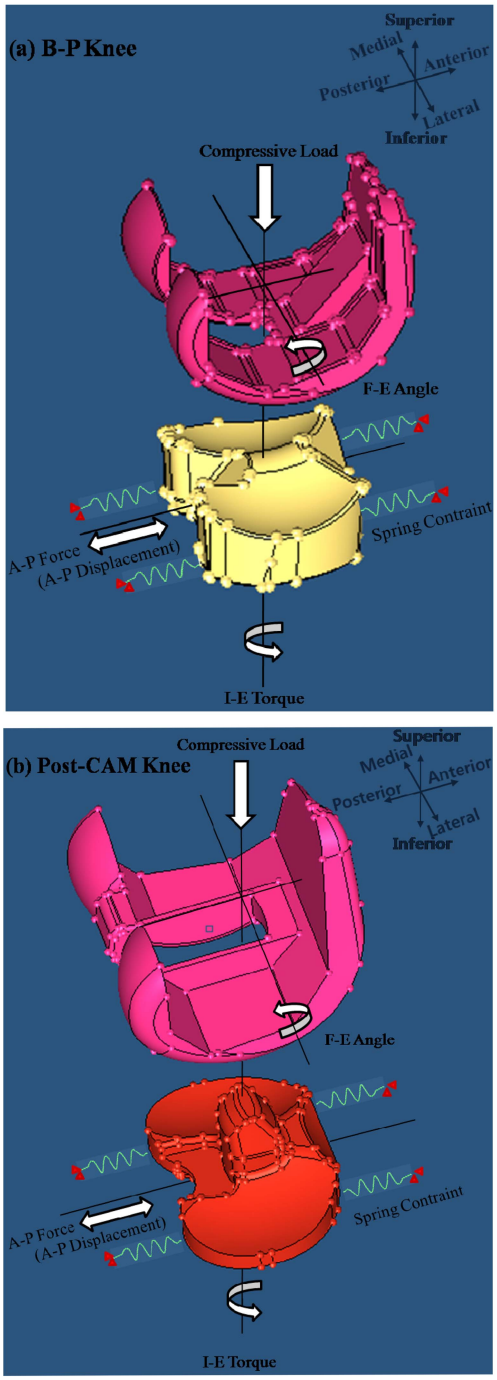

Fig. 4 Finite element models on the Endolab knee simulator illustrating force-control loading and displacement-control loading conditions for (a) B-P Knee and (b) Post-Cam Knee

optimized specifically for the mesh and loading conditions so that the kinematics and contact mechanics predicted were comparable with a fully deformable analysis.[17-19] The FE model reproduced the mechanical environment present in the Endolab knee simulator (Endolab Inc., Thansau/Rosenheim, Germany).

Simulated soft-tissue constraints present in the knee simulator, which consisted of a set of four springs to constrain the bearing in anterior-posterior (AP) displacement and internal-external (IE) rotation, and a spring elements designed to represent anatomical laxity, were reproduced in the model (Fig. 4).

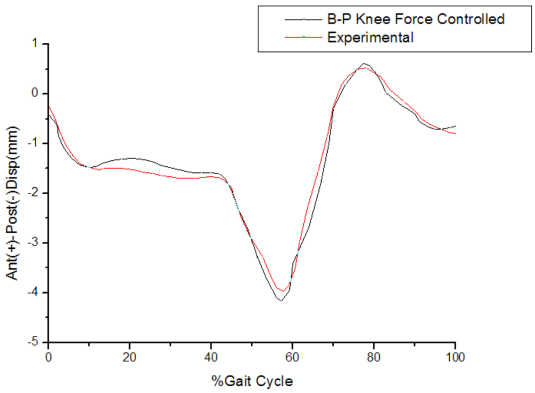

(a)

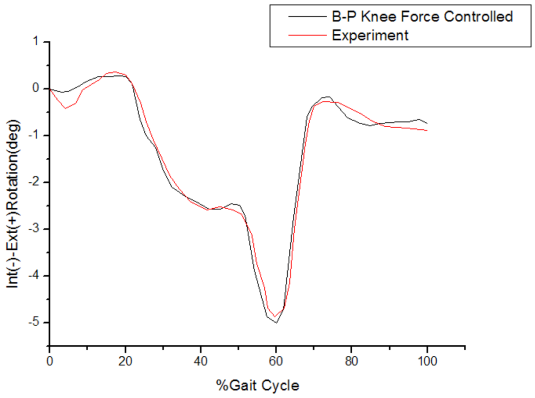

(b)

Fig. 5 (a) Experimental (Endolab knee simulator) and model-predicted anterior–posterior displacement as a function of gait cycle for the finite element model. (b) Experimental (Endolab knee simulator) and model-predicted internal-external rotation as a function of gait cycle for the finite element model

The femoral component was constrained in IE, medial–lateral (ML), AP, and varus-valgus (VV) degrees of freedom, while flexion extension and compressive load were applied (Fig. 4). The distal surface of the bearing was supported in the inferior–superior (IS) direction. Bearing tilt was constrained, and VV and ML degrees of freedom were free.

Two FE models were constructed based on the nature of the prescribed boundary conditions for both force-controlled and displacement-controlled conditions.

2.3 Femoral-bearing experimental validation

Experimental wear testing was performed on the Endolab knee simulator for 5 million gait cycles at a frequency of 1 cycle per sec (1 Hz). One sample of a cruciate-sacrificing B-P Knee implant was used. In this experiment, the force-controlled inputs used were nearly identical to ISO gait-loading conditions (ISO Draft Standard 14243-1).

The tibial component was aligned at 0° tilt and the femoral component was set with a 7° shift in flexion (towards hyper-extension). The neutral position for the experiment was defined as where a fully extended femoral component would settle statically on a horizontal tibial component under an applied vertical load.

The input profiles included an anterior-posterior load and internal-external torque applied to the bearing, and a flexion-extension angle and an axial force applied to the femoral component (Fig. 3). The bearing was allowed to translate along the anterior-posterior axis and rotate about a vertical axis through the center of the bearing.

The masses of the components are included but are small compared to the moving fixtures of the simulator. Due to the complexity, inertial effects, and resistance present in the simulator, it is unrealistic to model the entire structure. Simulated soft-tissue constraint present in the knee simulator consists of a set of four springs that constrain the bearing in anterior-posterior displacement and internal-external rotation.[20] For both the knee simulator and the FE model, the anterior-posterior translation resistance was 9.3 N/mm and the internal-external rotational resistance was 0.13 Nm/deg.

In the FE model, a center of rotation was defined directly between the medial and lateral condyles, and a set of four (medial and lateral) spring elements constrain the internal-external and anterior-posterior displacement as in the experimental simulator.

Kinematic trends and magnitudes, as well as the predicted contact area contours, were compared with the experimental data. Finally, contact stresses in B-P Knee and Post-Cam Knee were compared.

3. Results

3.1 Model Validation

Results from the FE model verification showed very good agreement between the predicted model and experimental kinematic data. Internal–external rotation and anterior–posterior translation are reported and showed a quiet positive agreement with the experimental data in trend and magnitude (Fig. 5).

The ranges in anterior-posterior and internal-external rotations from the experimental data were 4.7 mm and 3.9 degrees, respectively.

The predicted pattern of anterior-posterior motion matched closely with the experimental pattern during the entire gait cycle, but the analyses over-predicted peak data in the experimental pattern for most of the gait cycle. Overall, the predicted kinematics demonstrated excellent correlations with experimental data (Fig. 5).

The predicted internal–external rotation also matches the experimental data pattern for most of the gait cycle.

The predicted internal-external rotation was also well matched with the experimental data pattern for most of the gait cycle. During the initial 15% of the cycle, the predicted rotation did not agree with the experimental data in trend, but soon it found the right magnitude and trend.

3.2 Contact Stress

Fig. 6 Contact surface and pressure along the gait cycle A) Post-Cam Knee and B) B-P Knee.

Contact stress in the B-P Knee was greatest at 58% of gait cycle, compared with 62% of gait cycle in the Post-Cam Knee. In gait cycle analysis of the B-P Knee, the greatest contact stress was 38 MPa, which was one-third of the peak value for the Post-Cam Knee (105 MPa). Contact stress seemed to be the most influential component of axial force in both knee models. In the Post-Cam Knee, an asymmetric contact surface characteristic was most influential in IE torque, and axial force and IE torque reached peak values at 40% of the gait cycle. This was due to the effect of the

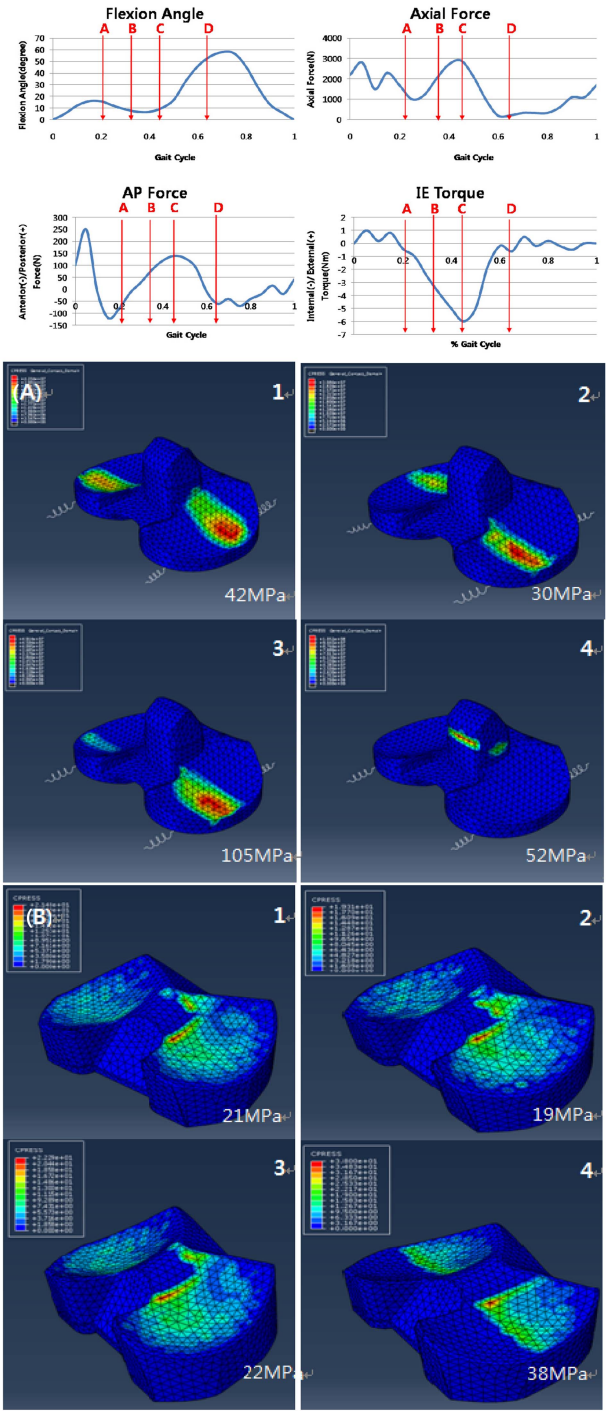

Fig. 6 shows the contact stress distribution on the bearing as gait cycle progresses

cam and was characteristic of the post-cam design. In overall, contact stress in B-P Knee design is lower than the one in Post-Cam Knee design. (Fig. 6)

3.3 Comparison of experimental and predicted contact area contours

Fig. 7 compares the wear contours predicted by the B-P Knee model with the experimental surface profilometry plots from gait cycles. Results for the model and experimental results show good qualitative agreement with respect to extent and periphery.

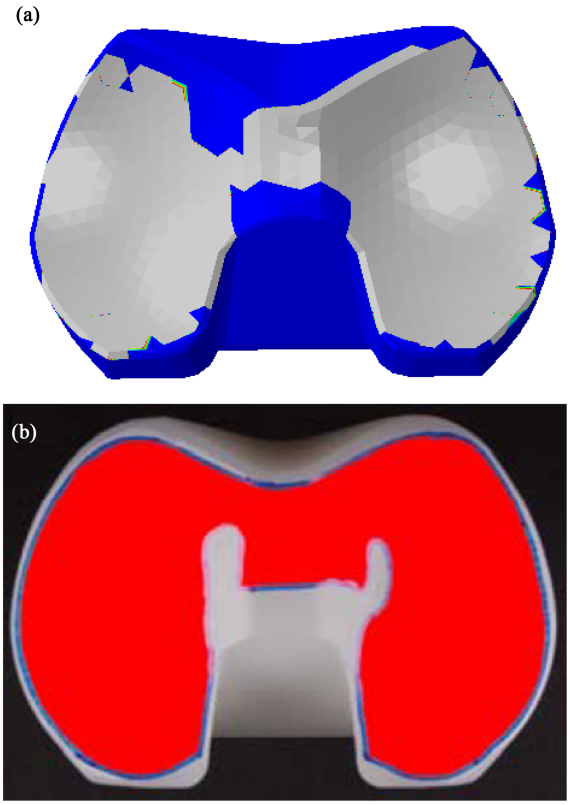

Fig. 7 Major contact area contour of the bearing: (a) Finite element model and (b) Experimental model

4. Discussion and Conclusions

Joint kinematics and contact mechanics significantly influence the long-term success of TKR. Polyethylene stresses and strains may predict wear or damage of a TKR component. Hence, a great deal of recent research has focused on determining the magnitude and distributions of stresses within the bearing. Implicit FE analyses have been used to determine contact mechanics in static positions or in a series of static positions representative of an activity cycle. Due to the inability of implicit methods to efficiently solve general force-controlled analyses, explicit FE methods have been investigated to simultaneously determine relative kinematics and contact stresses during dynamic loading. The present study is innovative in its combination of in vivo kinematics and FE analysis. Realistically modeling a total joint replacement construct with multiple moving contact surfaces is a formidable computational challenge. The current analysis assumes that the surgery introduced no abnormal alignment or soft tissue imbalance and that the geometry of the fabricated implant perfectly matches the Initial Graphics Exchange Specifications; i.e., contains no manufacturing defects. We specifically compared two posterior-stabilized designs, the B-P Knee in standard version and the Post-Cam Knee, over a standardized loading cycle using three-dimensional contact FE analysis.

Although Pendit et al. reported studies of surface geometry and post-cam,[21] their study did not address posterior sacrifice TKR. As far as we know, there are no studies comparing posterior sacrifice TKR designs.

Posterior-stabilized TKR is one of the most successful procedures in orthopedic surgery.[22,23] Recently, however, complications with the post-cam mechanism such as fracture or severe wear of the post have been reported.[24-26] For this reason, we compared the Post-Cam Knee with an alternative posterior-stabilized design, the B-P Knee. A previous study examined the process of rapid post-cam fracture, but only under static loading.[27] For a more accurate and complete description of the stresses involved, we analyzed the wear rate using explicit FE analysis during the gait cycle.

The choice of material strongly influences the accuracy of the contact model. Finite element studies of knee replacements have used both non-linear UHMWPE material models and linear material models.[8,9,12,14,15] A recent study determined the Young's modulus of UHMWPE to be 463 MPa using a miniature specimen shear punch test.[28] For an elastic foundation contact model a slightly lower value of Young's modulus is needed to produce the same total deformation, since pressures on surrounding elements do not contribute to the deformation of an element. This may explain why our experimental study produced a best-fit value for Young's modulus of 400 MPa. Furthermore, previous studies focused on either displacement control or force control,[18,19,29] whereas in the present study we used displacement control as the axial force and flexion extension, and force control for AP force and IE rotation. Results using this method agreed closely with the experimental results. However, the FE model was based on CAD implant geometry, and not on the manufactured part that was actually used in the experiment. Any geometrical deviation from manufacturing tolerances may introduce discrepancies between the simulation and experimental results. However, despite the limitations outlined above, this numerical approach can generate kinematic, contact-contour predictions that agree for the most part with experimental data. Our data show that polyethylene wear depends on both prosthetic kinematics and geometry, and shows a good agreement with a published report that the standard design is better in TKR kinematics than the post-cam design.[21] In other words if it is a posterior sacrifice design, the standard type is good for wear efficiency.

In conclusion, we showed that the contact stress of the B-P knee is lower than that of the Post-Cam knee, and confirmed the beneficial effect of high joint conformity. A deep groove in the B-P Knee design replaces the posterior stabilization feature in the Post-Cam Knee and may avoid the disadvantage of roll-back. The B-P Knee has the additional advantage of its light weight, being three times lighter than the Post-Cam Knee constructed of cobalt chrome, and naturally meets the requirements for implantation in the human body. The low conformity of the Post-Cam Knee prosthesis design was associated with greater contact stress. On the other hand, a high conformity curve in the design of the knee prosthesis increases the stress of contact even more during movement of the knee joint and decreases wear on the polyethylene bearing. Furthermore, the post-cam bearing has a calculable risk of fracture. Simulation testing saves time and costs less than physical contact testing and can incorporate more design parameters than was previously possible. Future studies will continue the FE analysis of the damage functions described herein. Injuries induced through mal-translation, mal-rotation, and varus tilt of the femoral component will be simulated and analyzed, because these are stresses that knee prostheses must withstand in vivo.

ACKNOWLEDGEMENT

This study was supported in part by Ministry of Knowledge Economy project (No.10032747).

REFERENCES

1. Won, C.-H., Rohatgi, S., Kraay, M. J., Goldberg, V. M., and Rimnac, C. M., "Effect of Resin Type and Manufacturing Method on Wear of Polyethylene Tibial Components," Clinical Orthopaedics and Related Research, Vol. 376, pp. 161-171, 2000.
2. Reeves, E. A., Barton, D. C., FitzPatrick, D. P., and Fisher, J., "Comparison of gas plasma and gamma irradiation in air sterilization on the delamination wear of the ultra-high molecular weight polyethylene used in knee replacements," Proc. IME. H. J. Eng. Med., Vol. 214, pp. 249-255, 2000.
3. Kim, Y. K. and Minh, H. L., "Laboratory-level Surgical Robot System for Minimal Invasive Surgery (MIS) Total Knee Arthroplasty," Int. J. Precis. Eng. Manuf., Vol. 12, No. 2, pp. 237-242, 2011.
4. Sathasivam, S., Walker, P. S., Campbell, P. A., and Rayner, K., "The effect of contact area on wear in relation to fixed bearing and mobile bearing knee replacements," J. Biomed. Mater. Res. Appl. Biomater., Vol. 58, pp. 282-290, 2001.
5. Lee, Y. S., Park, S. J., Song, E. K., Kim, J. S., and Kim, Y. H., "In Vivo Kinematics of a Cruciate Retaining Mobile-bearing Total Knee Arthroplasty," Int. J. Precis. Eng. Manuf., Vol. 12, No. 2, pp. 361-366, 2011.
6. Hood, R. W, Wright, T. M., and Burstein, A. H., "Retrieval analysis of total knee prostheses: a method and its application to 48 total condylar prostheses," J. Biomed. Mater. Res., Vol. 17, No. 5, pp. 829-842, 1983.
7. Paling, I. H., Schmalzried, T. P., and Callaghan, J. J., "Wear in total hip and knee replacements," J. Bone Jt. Surg. Am., Vol. 81, No. 1, pp. 115-36, 1999.
8. Bartel, D. L., Bicknell, V. L., and Wright, T. M., "The effect of conformity, thickness, and material on stresses in ultra-high molecular weight components for total joint replacement," J. Bone Jt. Surg. Am., Vol. 68, No. 7, pp. 1041-1051, 1986.
9. Bartel, D. L., Rawlinson, J. J., Burstein, A. H., Ranawat, C. S., and Flynn, W. F. J., "Stresses in polyethylene components of contemporary total knee replacements," Clin. Orthop., Vol. 317, pp. 76-82, 1995.
10. Kurtza, S. M., Pruittb, L, Jewettc, C. W., Crawfordc, R. P., Craneb, D. J., and Edidind, A. A., "The yielding, plastic flow, and fracture behavior of ultra-high molecular weight polyethylene used in total joint replacements," Biomater., Vol. 19, pp. 1989-2003, 1998.
11. Estupiñán, J. A., Bartel, D. L., and Wright, T. M., "Residual stresses in ultra-high molecular weight polyethylene loaded cyclically by a

rigid moving indenter in nonconforming geometries," J. Orthop. Res., Vol. 16, No. 1, pp. 80-88, 1998.

12. Sathasivam, S. and Walker, P. S., "Computer model to predict subsurface damage in tibial inserts of total knees," J. Orthop. Res., Vol. 16, No. 5, pp. 564-571, 1998.
13. Kurtz, S. M., Bartel, D. L., and Rimnac, C. M., "Post-irradiation aging affects the stresses and strains in UHMWPE components for total joint replacement," Clin. Orthop., Vol. 350, pp. 209-220, 1998.
14. Godesta, A. C., Beaugoninb, M., Haugb, E., Taylora, M., and Gregsona, P. J., "Simulation of a knee joint replacement during gait cycle using explicit finite element analysis," J. Biomech., Vol. 35, pp. 267-275, 2002.
15. Otto, J. K., Callaghan, J. J., and Brown, T. D., "Gait Cycle Finite Element Comparison of Rotating-Platform Total Knee Designs," Clin. Orthop. Relat. Res., No. 410, pp. 181-188, 2003.
16. Material Property Data, http://matweb.com
17. Halloran, J. P., Easley, S. K., Petrella, A. J., and Rullkoetter, P. J., "Comparison of deformable and elastic foundation finite element simulations for predicting knee replacement mechanics," J. Biomech. Eng., Vol. 127, pp. 813-818, 2005.
18. Hallorana, J. P., Petrellab, A. J., and Rullkoettera, P. J., "Explicit finite element modeling of TKR mechanics," J. Biomech., Vol. 38, pp. 323-331, 2005.
19. Knighta, L. A., Pala, S., Colemanc, J. C., Bronsona, F., Haiderd, H., Levinec, D. L., Taylorb, M., and Rullkoettera, P. J., "Comparison of long-term numerical and experimental total knee replacement wear during simulated gait loading," J. Biomech., Vol. 40, pp. 1550-1558, 2007.
20. Walker, P. S., Blunn, G. W., Broome, D. R., Perry, J., Watkins, A., Sathasivam, S., Dewar, M. E., and Paul, J. P., "A knee simulating machine for performance evaluation of total knee replacements," J. Biomech., Vol. 30, pp. 83-89, 1997.
21. Pandit, H., Ward, T., Hollinghurst, D., Beard, D. J., Gill, H. S., Thomas, N. P., and Murray, D. W., "Influence of surface geometry and the cam-post mechanism on the kinematics of total knee replacement," J. Bone Joint. Surg. [Br], Vol. 87-B, pp. 940-945, 2005.
22. Schai, P. A., Thornhill, T. S., and Scott, R. D., "Total knee arthroplasty with the PFC system : results at a minimum of ten years and survivorship analysis," J. Bone Joint. Surg. [Br], Vol. 80-B, pp. 850-858, 1998.
23. Rodriguez, J. A., Bhende, H., and Ranawat, C. S., "Total condylar knee replacement: a 20-year followup study," Clin. Orthop., Vol. 388, pp. 10-17, 2001.
24. Puloski, S. K. T., McCalden, R. W., MacDonald, S. J., Rorabeck, C. H., and Bourne, R. B., "Tibial post wear in posterior stabilized total knee arthroplasty: an unrecognized source of polyethylene debris," J. Bone. Joint. Surg. [Am], Vol. 83-A, pp. 390-397, 2001.
25. Mestha, P., Shenava, Y., and D'Arcy, J. C., "Fracture of the polyethylene tibial post in posterior stabilized (Insall Burstein II) total knee arthroplasty," J. Arthroplasty, Vol. 15, pp. 814-815, 2000.
26. Callaghan, J. J., O'Rourke, M. R., Goetz, D. D., Schmalzried, T. P., Campbell, P. A., and Johnston, R. C., "Tibial post impingement in posterior-stabilized total knee arthroplasty," Clin. Orthop., Vol. 404, pp. 83-88, 2002.
27. Nakayama, K., Matsuda, S., Miura, H., Higaki, H., Otsuka, K., and Iwamoto, Y., "Contact stress at the post-cam mechanism in posterior-stabilised total knee arthroplasty," J. Bone Joint Surg. [Br], Vol. 87-B, pp. 483-488, 2005.
28. Kurtza, S. M., Jewetta, C. W., Bergströma, J. S., Fouldsa, J. R., and Edidinb, A. A., "Miniature specimen shear punch test for UHMWPE used in total joint replacements," Biomater., Vol. 23, pp. 1907-1919, 2002.
29. Lanovaz, J. L. and Ellis, R. E., "Dynamic simulation of a displacement-controlled total knee replacement wear tester," Proc. IME. H. J. Eng. Med., Vol. 222, pp. 669-681, 2008.